
Powder Technology 283 (2015) 24-31

Development of 17-4PH stainless steel bimodal powder injection molding feedstock with the help of interparticle spacing/lubricating liquid concept

Bhimasena Nagaraj Mukunda^a, Berenika Hausnerova^{b,c,*}, Tirumani Srinivasan Shivashankar^a

^a Indo-US MIM Tec Pvt. Ltd., KIADB Industrial Area, Hoskote, Bangalore 562114, India

^b Department of Production Engineering Faculty of Technology, Tomas Bata University in Zlin, nam. T.G. Masaryka 5555, 760 01 Zlin, Czech Republic

^c Centre of Polymer Systems, University Institute, Tomas Bata University in Zlin, Nad Ovcirnou 3685, 760 01 Zlin, Czech Republic

ABSTRACT

Design of a powder injection molding (PIM) feedstock with proper selection of powder with unique particle size, particle shape and solid loading plays a significant role in controlling defects and distortion of PIM products. Using the concept of "interparticle spacing/volume fraction of lubricating liquid" 17-4PH stainless steel feedstocks with various bimodal powder combinations in thermoplastic polymer binder were designed and evaluated using both capillary and torque rheometers. Tendency to powder-binder separation, which is a factor indicating unacceptable distortions of sintered parts, is determined from the density variance during time- dependent viscosity measurement and thresholds in volume fraction of lubricating liquid as well as interparticle spacing parameters. The tailored feedstock with an optimum bimodal powder combination of coarse and fine particles exhibits suitable rheological performance with no evidence of separation and limited sintering distortion.

© 2015 Elsevier B.V. All rights reserved.

Keywords

Bimodal powder, Volume fraction of lubricating liquid, Interparticle spacing, Powder-binder separation, Distortion

* Corresponding author. Tel.: +420 57 603 5167.

E-mail address: hausnerova@ft.utb.cz (B. Hausnerova).

1. Introduction

Powder injection molding (PIM) is the process of manufacturing complex and precise metal and ceramic components. During molding, a feedstock is injected into the cavity at elevated pressure, temperature and shear rates varying between 10^2 and 10^5 s^{-1} [1]. The injection-molded products are then debound to remove a polymeric binder, and finally sintered at elevated temperatures to obtain the desired shape and dimensions.

Major defect in PIM components, which greatly affects the profile of the products (and in turn induces dimensional variations), is a distortion resulting from powder slumping after binder removal. It is governed by the inter-particle friction given by the particle size, shape and surface chemistry of the powder. Powder parameters as particle size, shape and its concentration in a powder-binder mixture (called feedstock) are the features dictating the final shrinkage and distortion of a PIM product. To minimize the dimensional shrinkage and distortion after debinding, the concentration of the powder in a feedstock is usually kept in the range of 50-80 vol.% depending on the powder and binder characteristics.

Several studies [2-4] have been carried out to understand the phenomenon of compact distortion in PIM components. Kipphut and German [2] indicated that the flow by viscous creep during thermal debinding is a major cause of a compact distortion. Liu et al. [3] investigated the effects of powder characteristic, solid loading, debinding atmosphere and heating rate on the compact deformation and found out that small particle size, irregular particle shape and high solid loading decrease the distortion in PIM products. On the other hand, faster heating rate induces distortion defects. The effects of powder loading of 60, 64, 68 and 72 vol.% on rheological properties, distortion, tolerance control, mechanical properties and microstructure were studied also for a feedstock based on 17-4PH gas atomized powder with 65/30/5 wt.% paraffin wax/EVA/stearic acid binder system [4]. Based on the results of tolerance control and compact distortion in tensile, rectangular, disc shaped and complex shape specimens 68 vol.% was selected as the optimum loading.

Distortion of the final PIM parts is also influenced by powder-binder separation occurring during injection molding step as a result of velocity gradients located close to the channel walls [5]. Currently, the investigation of the separation phenomenon is focused mainly on prediction of its onset and development during mold filling, which requires consideration of relevant processing factors and conditions and finding the method of quantitative determination of separation severity [6-8]. Further, Dihoru et al. [9] used a combination of capillary and torque rheometers, and developed neural network model to predict the maximum solid loading without powder-binder separation. The experimental study using neural network model suggests optimal loading for any feedstock 6-14% lower than the critical solid loading. The experimental study employed commercially available gas and water atomized powders (particle size ranging from 14 to 39 μm) blended in different ratios to study mono dispersed and bimodal feedstock characteristics. The study indicates that feedstocks made of blended powders have a higher risk of separation than those made from typical PIM powders. However, it was stated that the blended feedstocks are more stable than the feedstocks made of monodispersed powder particles of particle sizes 14 and 39 μm [9]. It should be noted that bimodal particle mixtures can be generally packed to higher densities than monosized particles. The key to improved packing largely depends on the particle size ratio [1, 10-13]. The larger the particle size ratio, the higher the packing density for any composition. The corresponding weight fraction of large particles for the maximum packing is 73.4% of larger particles and 26.6% of smaller particles [12].

Shivashankar et al. [14] proposed a material parameter called interparticle spacing parameter δ to predict powder-binder separation based on the powder characteristics as mean particle size (D_{50}), particle volume fraction (ϕ) and maximum particle fraction (ϕ_m):

$$\delta = D \left[\left(1 + \frac{1}{\phi} - \frac{1}{\phi_m} \right)^{1/3} - 1 \right] \quad (1)$$

The results confirmed that small interparticle spacing and/or low lubricating liquid increases powder-binder separation in a PIM feedstock. The interparticle distance is the unifying factor which combines the effects of the particle characteristics and the parameters such as viscosity, yield strength, or settling rate for a particle in a concentrated suspension.

Mukund and Shivashankar [15] have interpreted powder-binder separation in PIM feedstocks made of Fe 2%Ni, 17-4PH and Co-400 powders. The significant findings were the effect of solid loading on powder-binder separation via correlating it to the interparticle spacing δ and volume fraction of lubricating liquid ($1 - \phi / \phi_m$). Certain value (0.08) of the volume fraction of lubricating liquid represented the threshold for powder-binder separation.

The aim of the present research is to find an optimum 17-4PH bimodal powder combination exhibiting molding without generating defects and the least distortion during sintering among the selected powder combinations. Volume fraction of lubricating liquid and inter- particle spacing parameters will be tested for evaluation of powder- binder separation as a phenomenon indicating consecutive distortion. Additionally, cost comparison of all studied bimodal combinations with the monodispersed 17-4PH gas atomized powder ($D_{50} = 10.8 \mu\text{m}$) widely used in PIM industry will be performed.

2. Experimental

Five grades of 17-4PH gas atomized powder were chosen in the present research, Fig. 1. The particle size was measured using laser scattering method (Microtrac S3500) and the results are summarized in Table 1. Tap density of the individual powders and the chosen bimodal powder combinations was determined according to MPIF 46. Gas pycnometer (Accupyc 1330, Micromeritics) was used for determination of a pycnometer density of the feedstock samples.

The critical solid loading of all the chosen bimodal powder combinations was measured using Haake PolyLab Torque rheometer. It has a mixer capacity of 69 cm^3 with a mixing chamber divided into 3 segments and the temperature of each segment is monitored using inbuilt thermocouples. During mixing, the torque was recorded as a function of time. When the blades start to rotate (40 rpm), small amounts of powder and binder were alternately added into the mixing chamber. The loading level was increased in steps of 1 vol.% after 3 min of the stable torque cause. The powder addition was repeated until an abrupt increase in torque without stabilization was observed. The solid loading that led to this sudden increase was noted as the critical solid loading/ the maximum packing fraction (ϕ_m) for a given bimodal powder combination.

Capillary rheometer (Single bore, ITW Instron) was employed for the measurement of viscosity of the chosen bimodal feedstock formulations. The apparent viscosity is the ratio of apparent shear stress and apparent shear rate. The apparent shear rate is related to the volumetric flow rate, and the diameter of the capillary, while shear stress is related to the pressure drop in the capillary and its diameter/length ratio.

Powder-binder separation was studied using a combination of capillary rheometer and pycnometer. First, during the flow testing, the shear rate was fixed at 3001/s in order to evaluate the stability of the feedstock. The temperature was set at 180 °C. The homogeneity of feedstocks was checked with SEM before performing the stability test. The increase in the apparent viscosity during a constant shear rate test over a time would indicate powder-binder separation in a feedstock. Second, the pycnometer density was measured for both virgin feedstock and feedstock left in the barrel after the test. The higher the variation in density observed in the feedstock left in the barrel in comparison to the virgin feedstock, the higher the tendency to powder-binder separation during molding.

Rectangular samples of dimension (40 x 10 x 1.2) mm were molded using a CNC controlled screw type injection molding machine. The samples were thermally debound and sintered in a vacuum furnace with partial pressure under argon atmosphere. The molded specimens were rested at equal distance from both the ends using high thermal resistance alumina setters during both thermal debinding and sintering in an inert argon atmosphere. Fig. 2 shows the sketch of the distortion measured as the difference between the peak and the lowest point.

3. Results and discussion

Generally, there are three available methods to evaluate the maximum loading of a feedstock — fitting relative viscosity data with the suitable rheological model, density measurement, and mixing torque evaluation [1]. The latter is the most often used by researchers as well as practitioners (recently e.g. [16]). Thus, the critical levels of solid loading of the bimodal powder feedstocks were evaluated on a torque rheometer. A typical cause of the torque as a function of mixing time is demonstrated on (6/20) μm powder combination for concentrations increasing from 10 up to 72 vol.% (Fig. 3). With increasing loading level of the powder, the overall level of torque rises, but up to a critical concentration it always reaches the stable (constant) level. This is not the case with the highest loading (72 vol.%), where the torque is increasing with time as all the binders become locked in the interparticle spaces and the powder particles are in the direct contact offering higher resistivity to the flow.

Further, the density measurement has been also applied on the tested feedstocks. In that case the critical loading level is derived from the powder concentration value failing down from the theoretical line between densities of pure binder and powder. As it can be seen from the results obtained for (6/20) μm feedstock (Fig. 4), the density analysis coincides well with the results obtained from mixing torque if one takes into the account that at the critical point of density analysis, the air is trapped in the interparticle voids [1].

Third method available — fitting the relative viscosity data with rheological models — has not been applied on the bimodal feedstocks for two reasons. First, majority of available models containing the maximum loading parameter were established for monosized powders. Second, as it has been shown in the work of Honek et al. [17], an examination of the validity of models most often recommended in the literature [e.g. [1]] on experimental data for compounds based on powders varying in particle size distribution revealed ambiguous results. Overall, the maximum loading levels of PIM compounds established using these models corresponded to the powder characteristics: the highest value of maximum loading was predicted for the powder with a broad distribution of particle sizes, while the lowest value was attained for powder with a high portion of small particles. Nevertheless, contrary to the fact that several models fitted relatively well the flow data, the predicted values of the maximum volume fraction for the same powder varied (up to about 10 vol.%) with the model employed [17].

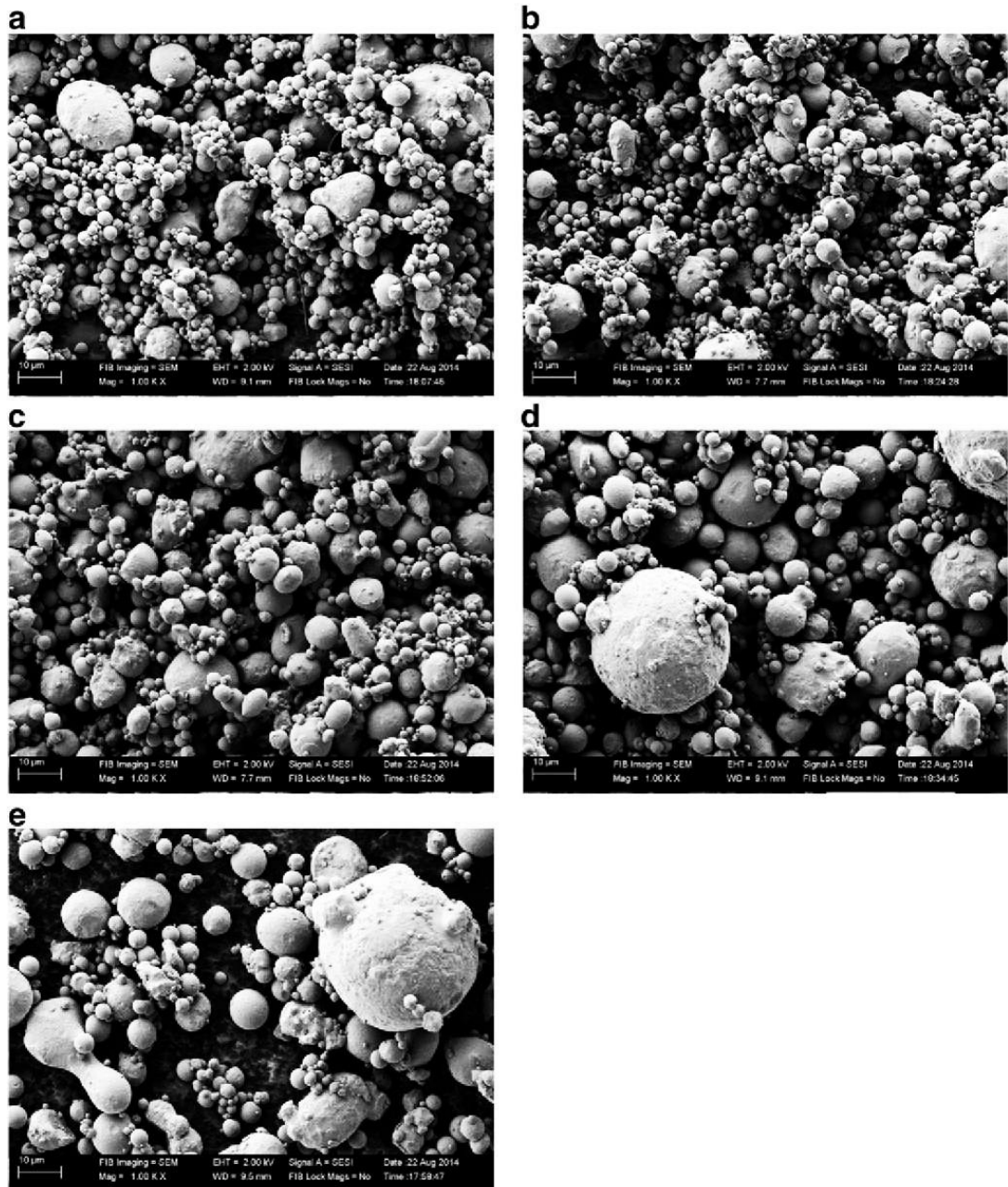


Fig. 1. SEM micrographs of 25/75 wt.% bimodal 17-4PH powders employed: (3.3/10.8) μm (a), (3.3/20) μm (b), (6/20) μm (c), (10.8/20) μm (c) and (10.8/45) μm (e).

The obtained bimodal powder tap densities are summarized in Table 2 together with the maximum (critical) solid loading of the bimodal powders. The tap density results indicate that an increase in the amount of coarser powder particles increases the packing density among all tested bimodal powder combinations. It was also observed that the packing of 75 wt.% of coarser particles and 25 wt.% of smaller particles gives the maximum packing density among the experimental weight fractions of bimodal powder combinations tested (75/25, 50/50 and 25/75 wt.%), which is in agreement with the results reported in literature [12].

| Table 1 Pycnometer and tap densities of selected 17-4PH powders. | | |
|--|---|--|
| Mean particle size D_{50} (μm) | Pycnometer density (g/cm^3) | Tap density (g/cm^3) |
| 3.3 | 7.80 | 4.1 |
| 6.0 | 7.78 | 4.3 |
| 10.8 | 7.85 | 4.6 |
| 20 | 7.88 | 4.8 |
| 45 | 7.88 | 5.2 |

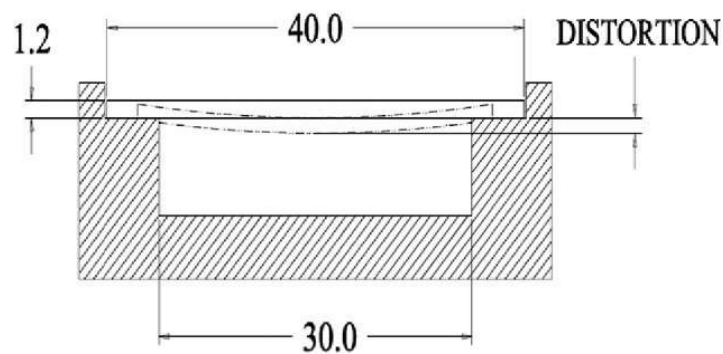


Fig. 2. Schema of a distortion measurement set-up.

Selected 25 finer/75 coarser wt.% bimodal feedstocks were mixed with a thermoplastic binder at two different solid loadings to investigate powder-binder separation and determine shape retention. Fig. 5 shows time dependency of an apparent viscosity at a constant shear rate 3001/s for (10.8/20) μm feedstock at 69 and 72 vol.% solid loadings. The latter exhibited an increase in apparent viscosity with time, whereas the constant viscosity as a function of time was observed for the feedstock loaded with 69 vol.% of powder. To avoid a figure crowding the constant shear rate test results for all bimodal feedstock combinations are summarized in Table 3 and those selected for the further analysis shown in combinations are summarized in Fig. 6.

From the same rheological testing the variation in density is derived from comparison of the density value obtained in the barrel and that of a virgin material. This parameter indicates the changes in the feedstock composition in terms of powder-binder separation. The lowest variation is observed for (6/20) μm feedstock loaded with 70 vol.% powder. Overall, the density data corresponds well with the stability/instability of viscosity in terms of the time. All feedstocks having viscosity increasing with time are characterized with density variation higher than 1%. Furthermore, the data confirms that binder content corresponding to the critical (maximum) solid loading, where relative viscosity approaches to infinity [1], deteriorates the stable flow in feedstock causing powder-binder separation.

The distortion also has an effect on component inability to meet typical PIM dimensional tolerance of $\pm 0.3\%$ [1,10-12]. Distortions of the bimodal feedstocks are shown in Fig. 7 together with the corresponding values for three monodispersed feedstocks for comparison. The feedstocks which exhibited an increase in apparent viscosity during constant shear rate test and higher variation in a barrel feedstock density could not be molded due to severe short fills and inconsistencies in molding. As shown in Fig. 7, the 70 vol.%

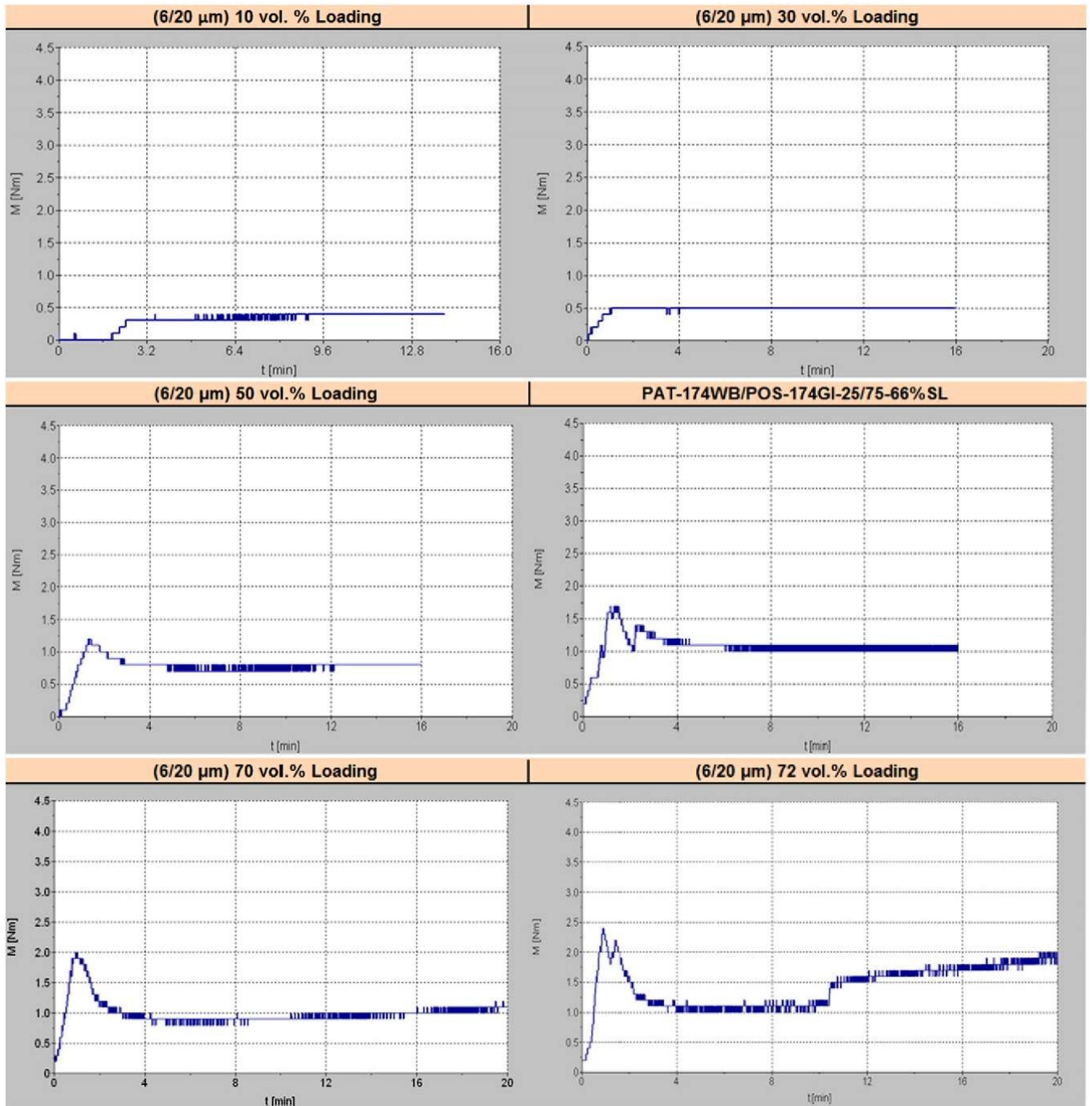


Fig. 3. Torque measurements for (6/20) μm feedstock.

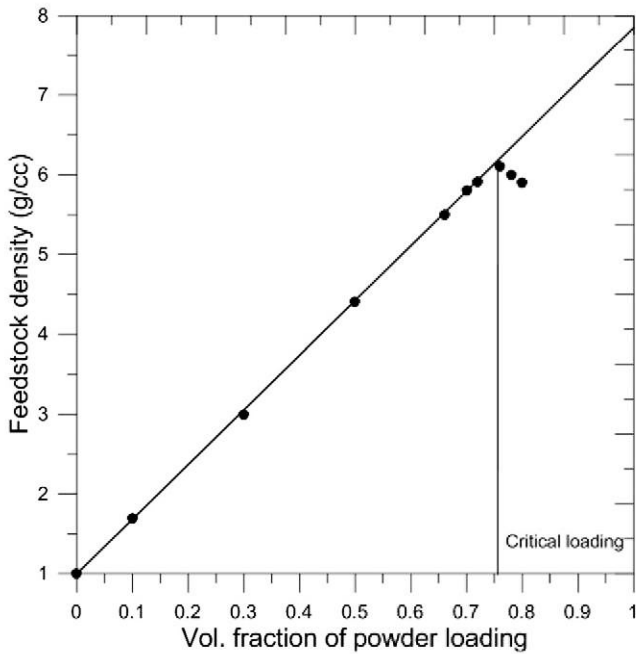


Fig. 4. Density analysis of the critical solid loading for (6/20) μm feedstock.

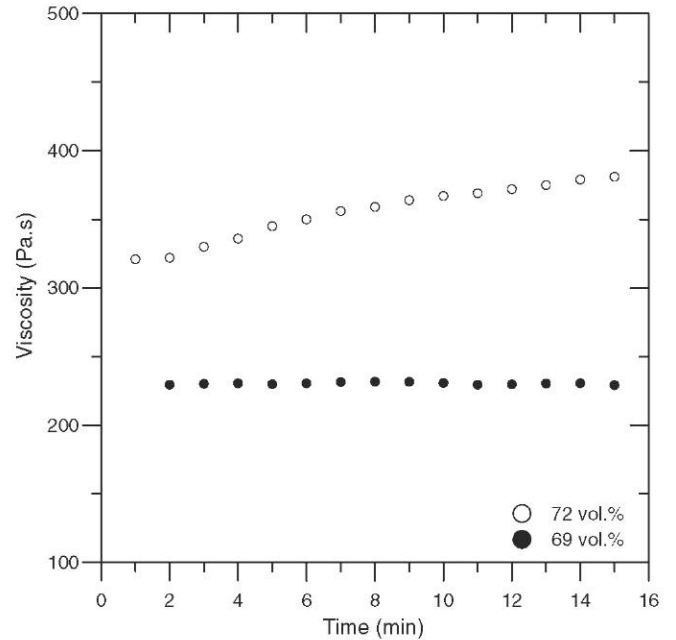


Fig. 5. Apparent viscosity of 17-4PH (10.8/20) μm bimodal feedstock at 69 and 72 vol.% loading as a function of time at constant shear rate of 3001/s.

bimodal combination of (6/20) μm manifests the lowest distortion of 3.46 mm as well as reproducibility in terms of a standard deviation (± 0.09) compared to other bimodal powder combinations studied. It should be noted that the obtained distortions of bimodal feedstocks correspond precisely to the values found for the particular monomodal powders, e.g. the distortion evaluated for (10.8/45) μm as (5.12 ± 0.34) μm arises from those obtained for feedstocks based on 10.8 μm and 45 μm filler if an additivity rule is applied for 25/75 wt.% ratio of the finer to the coarser powder.

Fig. 8 depicts interparticle spacing parameter δ computed according to Eq. (1) as a function of volume fraction of lubricating liquid ($1 - (\phi / \phi_m)$). With the reference to data in Table 3 and Table 4, a low amount of lubricating liquid accompanied with enhanced density variation results in the feedstocks being more prone towards powder-binder separation, which is in agreement with the qualitative explanation reported in [14,15]. The experimental data indicated a pronounced increase in apparent viscosity and variation in density of feedstock in a barrel in comparison to virgin feedstocks when the volume fraction of lubricating liquid ($1 - (\phi / \phi_m)$) is below the threshold of 0.08. This clearly indicates powder-binder separation. This was confirmed by molding specimens for all the chosen bimodal combinations with a volume fraction of lubricating liquid less than 0.08. The molded products had defects as short fills, stress marks and blisters which clearly indicate that there is an insufficient binder content in feedstocks resulting in discrepancies in flow behavior. Hence, the volume fraction of lubricating liquid is an indication of easier molding of PIM products with least or no defects. However, the threshold (0.08) derived for volume fraction of lubricating liquid in the present study is mainly applicable for the binder chemistry chosen in the study, and hence the same threshold may not be applicable for the feedstocks with different binder compositions.

Table 4 demonstrates also the applicability of the proposed interparticle spacing parameter δ to predict powder-binder separation of feedstocks containing bimodal powder particles. Interparticle spacing parameter is found to correlate well with the occurrence of a compact distortion and powder-binder separation in the present study. The maximum value of δ was found to be 0.66 μm in the case of (10.8/45) μm bimodal combination at 71 vol.% solid loading, whereas a minimum value of δ of 0.14 μm was

| Bimodal powder (μm) | Tap density (g/cm^3) | Critical solid loading (vol. %) |
|----------------------------------|--|---------------------------------|
| 3.3/10.8 | 4.49 | 70 |
| 10.8/20 | 4.87 | 76 |
| 10.8/45 | 5.26 | 78 |
| 3.3/20 | 4.55 | 75 |
| 6/20 | 4.59 | 76 |

| Bimodal powder (μm) | Solid loading (vol.%) | Density variation (%) | Flow stability |
|----------------------------------|-----------------------|-----------------------|--------------------------------------|
| 3.3/10.8 | 64 | 0.388 | Stable |
| 10.8/20 | 69 | 0.597 | Stable |
| 10.8/45 | 72 | 1.576 | Unstable, increase in app. viscosity |
| | 71 | 0.155 | Stable |
| 3.3/20 | 74 | 1.734 | Unstable, increase in app. viscosity |
| | 68 | 0.373 | Stable |
| 6/20 | 70 | 1.130 | Unstable, increase in app. viscosity |
| | 70 | 0.123 | Stable |
| | 72 | 1.524 | Unstable, increase in app. viscosity |

obtained for (3.3/20) μm feedstock at 70 vol.% solid loading. It can be noted from Eq. (1) and Fig. 8 that δ decreases with lower particle diameter D , and increases proportionately with higher particle diameter D for the same solid loading due to the increase in critical solid loading (ϕ_m) in the latter. Hence, the proposed parameter δ can be used for bimodal mixtures to calculate the interparticle distance between the powder particles as it is mainly driven by powder particle parameters as particle diameter (D), solid loading (ϕ) and critical solid loading (ϕ_m). Any feedstock with δ less than 0.5 μm is proposed for successful PIM, Fig. 8. From this point of view, bimodal combinations of (3.3/20) μm at 64 vol.%, (3.3/10.8) μm at 64 vol.% and (6/20) μm at 70 vol.% with δ of 0.21, 0.33 and 0.35, respectively, seem to be the feedstocks fulfilling the purpose. Low δ reduces the interparticle spacing resulting in lowering distortion as presented.

Though other combinations as (10.8/20) μm and (10.8/45) μm may reduce the cost up to 12-14%, they failed to impart low distortion due to the higher interparticle spacing. On the other hand, the cost of the bimodal combinations of (3.3/10.8) μm and (3.3/20) μm would be 3 to 4 times higher than that of the standard monodispersed 17-4PH powder due to the higher cost of finer grade powder (3.3 μm) used in the formulations. In this respect, the combination of (6/20) μm found to be 10% lower in cost and having low particle spacing along with significant reduction in distortion in comparison to the monodispersed 17-4PH powder as well as to the other bimodal feedstocks tested. Furthermore, sintered density of this feedstock was found to be 7.73-7.75 g/cm^3 with porosity of 0.4%, while the most unsuitable (10.8/45) μm feedstock had a density of 7.67-7.70 g/cm^3 and porosity of 1.44%, Table 5 and Fig. 9. In addition, the microstructural analysis of products molded with optimum bimodal feedstock with powder (6/20) μm was compared with that of monodispersed (10.8) μm gas atomized powder (Fig. 10). It was found that both the monodispersed powder and optimum bimodal powder combination are having the same heat treated martensitic structure

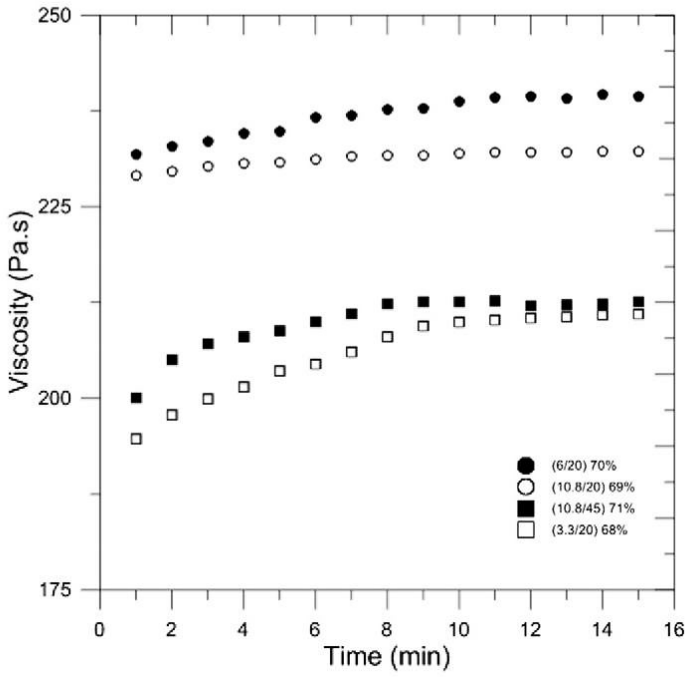


Fig. 6. Apparent viscosity of 17-4PH bimodal feedstocks at optimal loading as a function of time at a constant shear rate of 3001 /s.

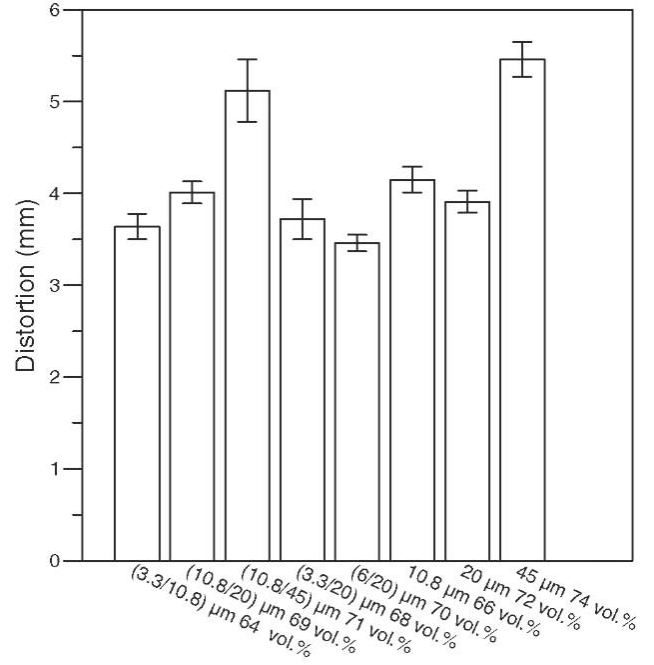


Fig. 7. Distortions observed in feedstocks molded with the selected bimodal and monodispersed powder combinations.

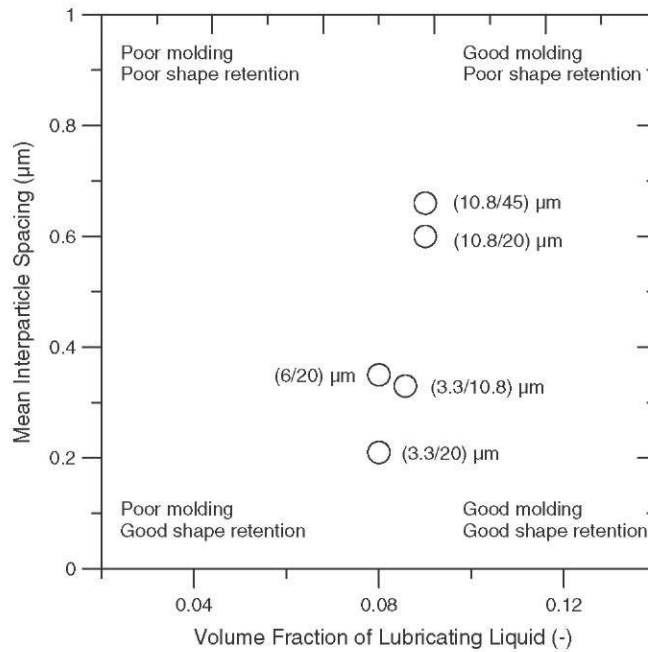


Fig. 8. Mapping of interparticle spacing parameter and volume fraction of lubricating liquid to intercept an optimum, powder-binder separation, and distortion regions.

Table 4
Analysis of an optimum bimodal powder combination.

| Bimodal powder (μm) | Solid loading (vol.%) | Volume fraction of lubricating liquid | Distortion (mm) | Interparticle spacing (μm) | Cost change |
|----------------------------------|-----------------------|---------------------------------------|-------------------------|---|-------------|
| 3.3/10.8 | 64 | 0.090 | 3.64 | 0.33 | 4x |
| 10.8/20 | 69 | 0.090 | 4.01 | 0.60 | 0.88 x |
| | 72 | 0.050 | Not molded ^a | 0.34 | NA |
| 10.8/45 | 71 | 0.090 | 5.12 | 0.66 | 0.86 x |
| | 74 | 0.050 | Not molded | 0.37 | NA |
| 3.3/20 | 68 | 0.080 | 3.72 | 0.21 | 3.5 x |
| | 70 | 0.070 | Not molded | 0.14 | NA |
| 6/20 | 70 | 0.080 | 3.46 | 0.35 | 0.90 x |
| | 72 | 0.050 | Not molded | 0.23 | NA |

^a Not molded means attempted to be molded but ended up with defects as short fill, stress marks and blisters.

Table 5
Sintered density and porosity of selected bimodal powder feedstocks as well as a monosized powder feedstock for comparison.

| Bimodal Powder (μm) | Solid loading (vol.%) | Sintered density (g/cm^3) | Porosity (%) |
|----------------------------------|-----------------------|---|--------------|
| 3.3/10.8 | 64 | 7.70-7.76 | 0.44 |
| 10.8/20 | 69 | 7.71-7.76 | 0.48 |
| 10.8/45 | 71 | 7.67-7.70 | 1.44 |
| 3.3/20 | 68 | 7.70-7.72 | 0.89 |
| 6/20 | 70 | 7.73-7.75 | 0.40 |
| 10.8 | 66 | 7.68-7.69 | 0.76 |

with the grain size number ranging from 5.5 to 6 according to ASTM E112 Standard. Finally, sintered products were examined to evaluate the Rockwell hardness for both monodispersed 100% gas atomized powder (10.8 μm) and optimum bimodal 17-4PH feedstock (6/20) μm and it reached the values 35.82-36.83 HRC and 34.5635.50 HRC, respectively, with no statistically significant difference between the two feedstocks performed using '2 Sample t' test method of a test hypothesis.



Fig. 9. Surface porosity of 70 vol.% (6/20) μm and 71 vol.% (10.8/45) μm bimodal powder feedstocks.

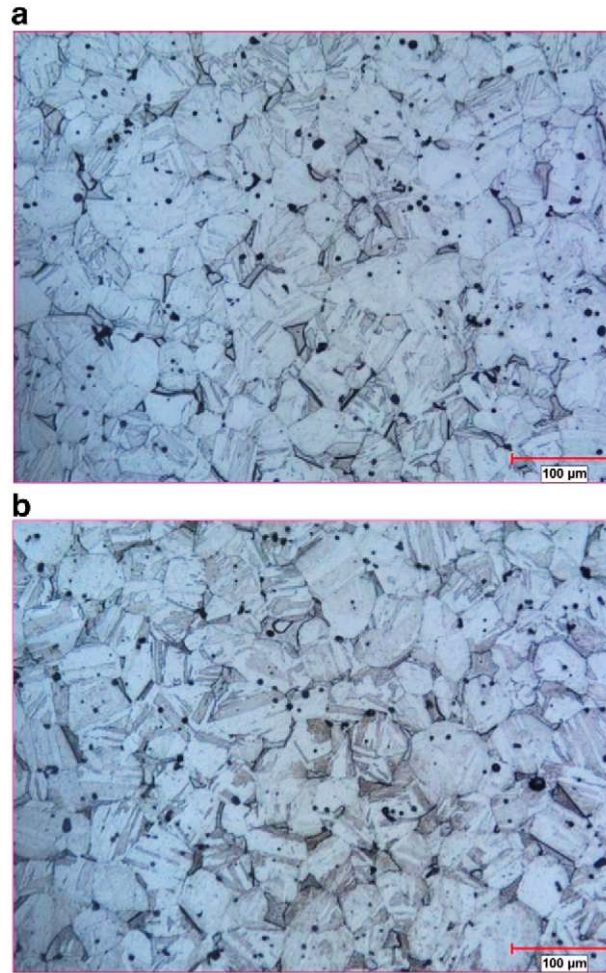


Fig. 10. Microstructural analysis of optimum bimodal (6/20) μm 17-4PH feedstock (a) compared with the monosized (10.8 μm) gas atomised powder (b).

4. Conclusion

The presented study interprets the ability of the bimodal powder feedstocks to improve the shape retention of PIM parts at simultaneous cost efficiency. Determination of packing density of all bimodal powder feedstocks tested resulted in the selection of 25/75 wt.% of finer/coarser powders for further analysis. It was found that bimodal feedstocks are stable against powder-binder separation when the volume fraction of lubricating liquid reaches the threshold of 0.08 (the value reported also for unimodal powders). Further, it has been found that the interparticle spacing higher than 0.5 μm endorses distortions during sintering. Among all tested 17-4PH bimodal powder combinations, the 70 vol.% feedstock containing (6/20) μm powders proved to be the most suitable in terms of powder-binder separation, shape retention characteristics (having a distortion of 3.46 mm) with the highest sintered density up to 7.75 g/cm^3 and the porosity of 0.4%. The derived bimodal combination can also reduce the powder cost up to 10% in comparison with the monosized powder grade of 17-4PH gas atomized powder used currently in the PIM industry.

Acknowledgments

G.S. Ananthapadmanabha is acknowledged for the help with the experimental. The author B.H. would like to acknowledge the support of Operational Program Research and Development for Innovations co-funded by the ERDF and the National Budget of Czech Republic, within the framework of project Centre of Polymer Systems (reg. number: CZ.1.05/2.1.00/03.0111).

References

- [1] R.M. German, A. Bose, Injection Molding of Metals and Ceramics, second ed, 1997. (Princeton, New Jersey).
- [2] C.M. Kipphut, R.M. German, Powder selection for shape retention in powder injection molding, *Int. J. Powder Metall.* 27 (1991) 117-124.
- [3] X.Q. Liu, Y.M. Li, J.L. Yue, F.H. Luo, Deformation behavior and strength evolution of MIM compacts during thermal debinding, *Trans. Nonferrous Metals Soc. China* 18 (2008) 278-284.
- [4] Y. Li, L. Li, KA Khalil, Effect of powder loading on metal injection molding of stainless steels, *J. Mater. Process. Technol.* 183 (2007) 432-439.
- [5] M. Thornagel, MIM simulation: a virtual study on phase separation, European Powder Metallurgy Association, *Proc. Eur. Powder Metall.* (2009) 135-140.
- [6] M. Jenni, L. Schimmer, R. Zauner, J. Stampfl, Morris, Quantitative study of powder binder separation of feedstocks, *PIM Int.* 2 (2008) 50-55.
- [7] LJiranelc, B. Hausnerova, T. Hartwig, Community Design 001704974, Office for Harmonization in the Internal Market, Alicante, 2010.
- [8] B. Hausnerova, D. Sanetnik P. Ponizil, Surface structure analysis of injection molded highly filled polymer melts, *Polym. Compos.* 34 (2013) 1553-1558.
- [9] L.V. Dihoru, L.N. Smith, R.M. German, Experimental study and neural network modeling of the rheological behavior of powder injection molding feedstocks formed with bimodal mixture, *Powder Metall.* 43 (2000) 31 -36.
- [10] B.O. Rhee, C.I. Chung, Effects of binder characteristics on binder separation in powder injection molding, *Proc. Powder Inject. Mold. Symp* 1992, pp. 135-153.
- [11] A. Mannschatz, S. Höhn, T. Moritz, Powder-binder separation in injection molded green parts, *J. Eur. Ceram. Soc.* 30 (2010) 2827-2832.
- [12] R.M. German, Particle Packing Characteristics, Metal Powder Industries Federation, Princeton, New Jersey, 1989.
- [13] B. Hausnerova, P. Saha, J. Kubat, Capillary flow of hard-metal carbide compounds, *Int. Polym. Proc.* 14 (1999) 254-260.
- [14] T.S. Shivashankar, R. Enneti, S.J. Park, R.M. German, S. Atre, The effects of material attributes on powder-binder separation phenomena in powder injection molding, *Powder Technol.* 243 (2013) 79-84.
- [15] B.N. Mukund, T.S. Shivashankar, Effect of particle spacing on shape retention phenomena in powder injection molding, European Powder Metallurgy Association, *Proc. Eur. Powder Metall.* 2013, pp. 375-384.
- [16] J.P. Choi, H.G. Lyu, W.S. Lee, J.S. Lee, Investigation of the rheological behavior of 316L stainless steel micro-nano powder feedstock for micro powder injection molding, *Powder Technol.* 261 (2014) 201-209.

[17] T. Honelk B. Hausnerova, P. Saha, Relative viscosity models and their application to capillary flow data of highly filled hard-metal carbide powder compounds, Polym. Compos. 26 (2005) 29-36.